Journal of Alloys and Compounds 500 (2010) L17–L21

Contents lists available at ScienceDirect

Journal of Alloys and Compounds

journal homepage: www.elsevier.com/locate/jallcom

Short communication

Development of a wet chemical method for the synthesis of arrayed ZnO nanorods

Shao-Hwa Hu[a], Yi-Chuan Chen[b], Chyi-Ching Hwang[b,*], Cheng-Hsiung Peng[c], Dah-Chuan Gong[a]

[a] Department of Industrial and Systems Engineering, College of Electrical Engineering and Computer Science, Chung Yuan Christian University, Chungli, Taoyuan 320, Taiwan, ROC
[b] Department of Applied Chemistry and Materials Science, Chung Cheng Institute of Technology, NDU, Dasi, Taoyuan 335, Taiwan, ROC
[c] Department of Chemical Engineering and Materials Science, Ming Hsin University of Science and Technology, Hsinfeng, Hsinchu 304, Taiwan, ROC

ARTICLE INFO

Article history:
Received 19 January 2010
Received in revised form 23 March 2010
Accepted 30 March 2010
Available online 8 April 2010

Keywords:
Wet chemical
ZnO
Nanorods
Photoluminescence

ABSTRACT

A two-step wet chemical process with economic and practical advantages was developed to prepare arrayed ZnO nanorods on glass substrates using zinc acetate dihydrate ($Zn(CH_3COO)_2{\cdot}2H_2O$, $ZnAc_2$) and monoethanolamine ($NH_2CH_2CH_2OH$, MEA) as raw materials. The proposed method includes the pre-deposition of a thin ZnO seed layer using the sol–gel technique and the subsequent hydrothermal growth of ZnO nanorods at 130 °C for 2 or 4 h. The synthesis process was monitored using X-ray diffraction (XRD), Fourier transformation infrared (FTIR) spectroscopy, atomic force microscopy (AFM), scanning electron microscopy (SEM) and transmission electron microscopy (TEM). The ZnO nanorods exhibited a diameter of 25–75 nm with an aspect ratio ranging from 10 to 50 after growing for 4 h. Each ZnO nanorod was confirmed to be a single crystal with a wurtzite structure and grow along the [0 0 0 2] direction during the hydrothermal process. Photoluminescence (PL) measurements confirmed that the ZnO nanorods exhibited a near-UV emission at ~380nm together with a green emission that was centered at ~500 nm. We note that the PL properties may be affected by the hydrothermal time.

1. Introduction

Nanostructured zinc oxide (ZnO) is of interest in the optoelectronic, piezoelectric, sensor, biomedical and electro-chemical fields because of its interesting characteristics, such as a direct band gap of 3.37 eV, a large exciton binding energy of 60 meV at room temperature, transparent conductivity, non-centrosymmetric symmetry, bio-safty and bio-compatibility properties [1–3]. Hence, nanostructured ZnO with different morphologies, such as particles, rods/fibers/wires, thin films, and multipods, has attracted substantial attention from multiple researchers [4]. For example, arrayed one-dimensional (1D) ZnO crystallites have frequently been cited for their potential in electronic and optoelectronic applications [3,5–9].

Two major categories of techniques have been developed for the synthesis of 1D ZnO arrays, namely, vapor-phase processes and the wet chemical route. Various vapor-phase processes (for example, vapor–liquid–solid epitaxial (VLSE) growth [10], metal–organic chemical vapor deposition (MOCVD) [11], and thermal evaporation [7,12] have been developed for the synthesis of 1D ZnO arrays. However, expensive and complicated equipments is required in these processes to guarantee suitably rigorous conditions, such as high temperatures (≥400 °C), low pressures and adequate atmospheric control, thus limiting the available substrate materials and large-scale production of the arrayed 1D ZnO arrays [3,9]. On the other hand, the wet chemical route is now a promising option for large-scale 1D ZnO arrays fabrication on arbitrary substrates at low cost and under remarkably low temperature conditions [3,6,8,9]. The morphology and characteristics of the wet chemical-derived 1D ZnO crystallites can be varied by changing the starting materials, the reactant concentrations, procedural details, and growth temperature and time. Vayssieres [5] developed a template-less and surfactant-free aqueous method to grow arrayed ZnO nanorods/nanowires on various kinds of substrates through the thermal decomposition of a Zn^{II} amino complex at 95 °C for several hours using the raw materials of zinc nitrate hexahydrate ($Zn(NO_3)_2{\cdot}6H_2O$) and methenamineod ($C_6H_{12}N_4$), which have since become the most common formulation for the hydrothermal growth of ZnO nanorods. Greene et al. [6] used a two-step process to produce ZnO nanowire arrays on a 4-in. Si(1 0 0) wafer and a flexible 5-cm-diameter polydimethylsiloxane (PDMS) substrate. A ZnO seed layer was prepared from a sol–gel reaction using a methanolic solution of $Zn(CH_3COO)_2{\cdot}2H_2O$ and NaOH prior to the hydrothermal treatment, thereby resulting in an improved alignment of the resultant ZnO arrays. Yi et al. [3] employed the same two-step process for growing ZnO nanorods on polyethylene terephthalae (PET) and verified that

* Corresponding author. Tel.: +886 3 3891716x114; fax: +886 3 3892494.
E-mail address: chyichinghwang@gmail.com (C.-C. Hwang).

0925-8388/$ – see front matter © 2010 Elsevier B.V. All rights reserved.
doi:10.1016/j.jallcom.2010.03.235

the ZnO seeds are indispensable for the aligned growth of ZnO nanorods with a high population density. Therefore, the alignment of the ZnO seeds was thought to be substrate-independent and was believed to occur on flat surfaces regardless of their crystallinity or surface chemistry. However, Wang et al. [9] claimed that in the $Zn(NO_3)_2{\cdot}6H_2O$–$(NH_2)_2CS$–NH_4Cl–NH_4OH aqueous solution with the assistance of ultrasonic treatment, aligned tower-like or tube-like ZnO crystals can be fabricated on different substrates by self-assembly without a layer of prepared coats or seeds.

In this preliminary work, a formulation composed of $Zn(CH_3COO)_2{\cdot}2H_2O$ and monoethanolamine ($NH_2CH_2CH_2OH$), which are commonly used in the sol–gel technique for preparing transparent conducting ZnO thin films [13–15], was used to develop an alternative wet chemical process for the synthesis of aligned ZnO nanorods on glass substrates and to avoid the unwanted ions or impurity (such as Na^+, Cl^- or the derivatives of $(NH_2)_2CS$) in the resulting products. The development and the details of the alternative process will be described in this paper. Moreover, the effect of the growth time on the product properties was investigated and the possible formation mechanism for the as-prepared ZnO nanorods will be discussed.

2. Experimental procedure

Analytical-grade of zinc acetate dihydrate ($ZnAc_2$) and monoethanolamine (MEA) were selected as starting materials (Aldrich, USA). The $ZnAc_2$ was the source of the Zn^{2+} cation, and MEA acted as both a stabilizer and mineralizer. Silica glass ($2.5 \times 2.5\,cm^2$) was used as the substrate material, which was cleaned using a 5% H_2SO_4 aqueous solution, then rinsed ultrasonically in acetone and deionized water, and finally dried in a vacuum oven. A two-step process was applied to prepare arrayed ZnO nanorods on glass substrates, which included the pre-formation of a thin ZnO seed layer using a sol–gel technique and the subsequent hydrothermal growth of ZnO rods. In the first step, anhydrous ethanol was used as the solvent instead of other alcohols (such as methanol, 2-methoxyethanol, or isopropanol) or water due to considerations of safety, practicability and spreading behavior. Ethanolic $ZnAc_2$ was slowly added to the MEA–ethanol solution with stirring. A 1.0 molar ratio of $ZnAc_2$ to MEA was maintained, and the concentration of $ZnAc_2$ was 0.1 M. The mixed solution was refluxed with stirring at 60 °C for 2 h to yield a clear and homogeneous solution, which served as the precursor sol. Subsequently, the precursor sol was placed on the glass substrate and spun at 3000 rpm for 30 s to form a thin layer of dried precursor as a result of the centrifugal force and convective evaporation during the spin-coating process. The coated substrates were preheated at 300 °C for 10 min on a hot plate to transform the dried precursor into ZnO seeds and to guarantee adhesion of the as-formed ZnO seeds to the substrate surface. The spin coating and preheating procedure was repeated twice to guarantee a uniform distribution and adequate coverage of the ZnO seeds on the substrates. In our follow-up hydrothermal step, the substrate deposited with ZnO seeds was put into an autoclave and submerged in a mixed aqueous solution of 0.02 M $ZnAc_2$ and 0.04 M MEA at 130 °C for 2 or 4 h to promote the growth of arrayed rods on the ZnO seeds. After the hydrothermal process, the resultant product grown on the substrate was rinsed with deionized water and dried in a vacuum oven.

The resulting phase formation was identified by X-ray diffraction (XRD, SIEMENZ D-5000) with Cu-Kα_1 radiation ($\lambda = 0.15406$ nm). Morphological features of the samples were observed using scanning electron microscopy (SEM, Joel JSM-T330A). The roughness of the seed layer was characterized by atomic force microscopy (AFM, SPA 400). Fourier transform infrared spectroscopy (FTIR) measurements, in which the samples were scrapped off the substrates and dispersed in KBr pellets, were carried out with a Nicolet-870 spectrometer in transmittance mode. The resulting nanostructure together with the corresponding selected area electron diffraction (SAED) region was imaged using transmission electron microscopy (TEM, Hitachi H-7100). Photoluminescence (PL) spectra were measured at room temperature using a HeGd laser with a wavelength of 325 nm as the excitation source.

3. Results

Fig. 1 shows the XRD spectra of the glass substrate, the as-coated precursor on the substrate, the deposited film after preheating, and the as-obtained products after hydrothermal growth at 130 °C for 2 and 4 h. Judging from Fig. 1(a), it is suggested that the substrate material seemed to be amorphous in nature. The XRD spectra in all samples exhibits the same amorphous hump in the range of 20–30°, which possibly originate from the standard glass substrate. The XRD spectrum shown in Fig. 1(b) is similar to the diffraction

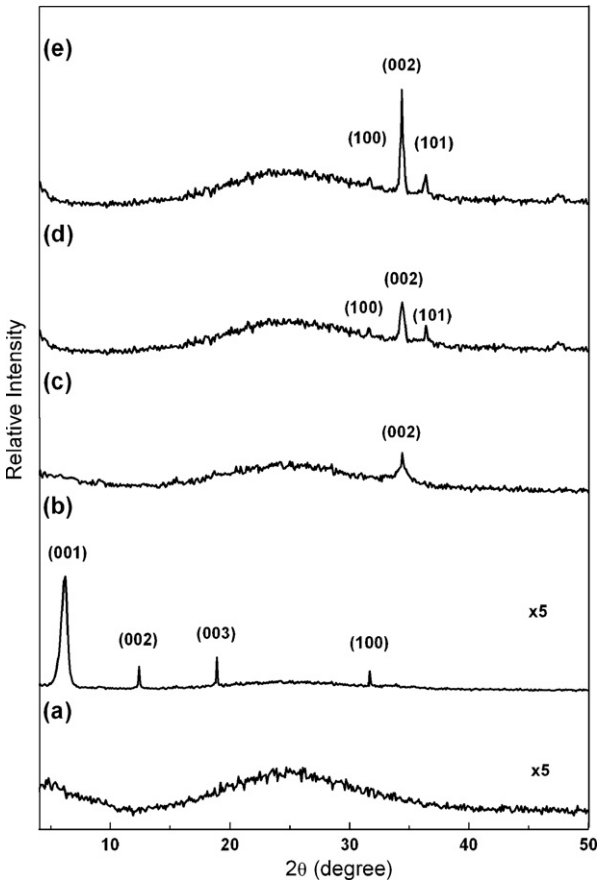

Fig. 1. XRD patterns of (a) silica glass substrate, (b) as-coated precursor on substrate, (c) deposited film after preheating, and as-obtained products after grown hydrothermally at 130 °C for (d) 2 h and (e) 4 h.

pattern of the compound, namely layered basic zinc acetate (LBZA, $Zn_5(OH)_8(CH_3COO)_2{\cdot}2H_2O$), as reported by Hosono et al. [16]. The precursor sol, which was coated on the substrate and dried in air by spin coating, was transformed into LBZA. As shown in Fig. 1(c), only a weak (0 0 2) characteristic peak at 34.4° belonging to Wurzite-type ZnO was observed (JCPDS 89-1397), indicating that the LBZA was converted to ZnO seeds with the preferred *c*-axis orientation after preheating at 300 °C. As shown in Fig. 1(d) and (e), although two other peaks corresponding to (1 0 0) and (1 0 1) planes were also recorded, the (0 0 2) diffraction peak was the most intensive. These results suggest that the ZnO nanorods grow mainly along the *c*-axis direction during the hydrothermal process, a fact that can be attributed that the minimum value of the surface free energy of the ZnO (0 0 2) plane during the growth stage [17]. In addition, the relative intensity of the ZnO (0 0 2) diffraction peak increased as the hydrothermal time was increased from 2 to 4 h, which may be related to both the preference for crystal growth and the enhancement of crystalline quality.

Fig. 2 shows the IR spectra for the dried precursor sol, the deposited film after preheating and the as-grown product. In Fig. 2(a), the strong and broad band from 3700 to 2800 cm^{-1} corresponds to the O–H group. The two bands located at ~1700 and ~1400 cm^{-1} were assigned to the asymmetric and symmetric COO– stretching vibration modes, respectively, which are characteristic of the acetate group. Absorption bands in the range of 1050–750 cm^{-1} indicate the binding of R-CH_2OH and NH_2-CH_2. The above data are based on reports from the literature [18]. In Fig. 2(b), all of the aforementioned bands almost disappeared after the deposited precursor film had been preheated at 300 °C. Moreover, a new band appeared at ~500 cm^{-1} (Fig. 2(b)), which can

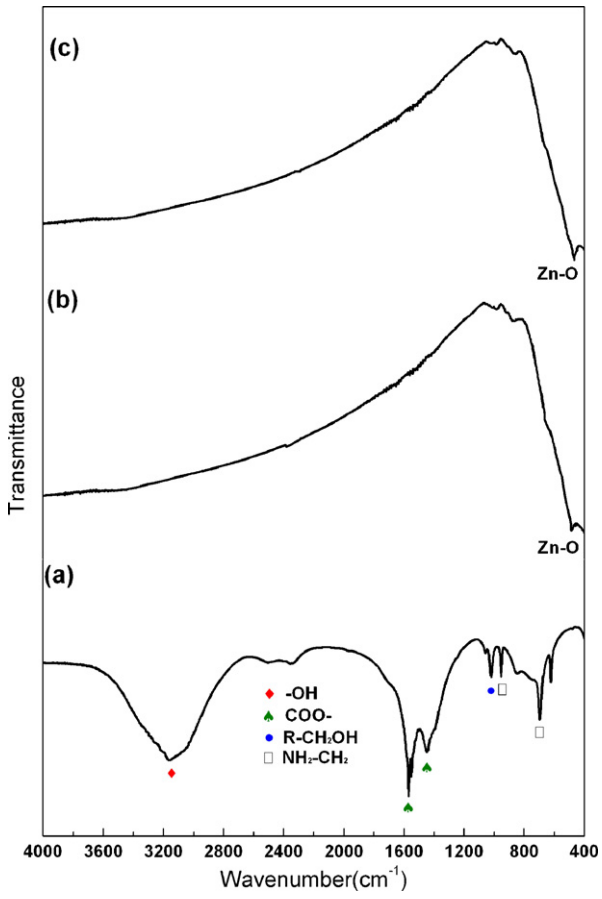

Fig. 2. FTIR spectra of (a) dried precursor, (b) deposited film after preheating, and (c) as-grown product after hydrothermal growth for 4 h.

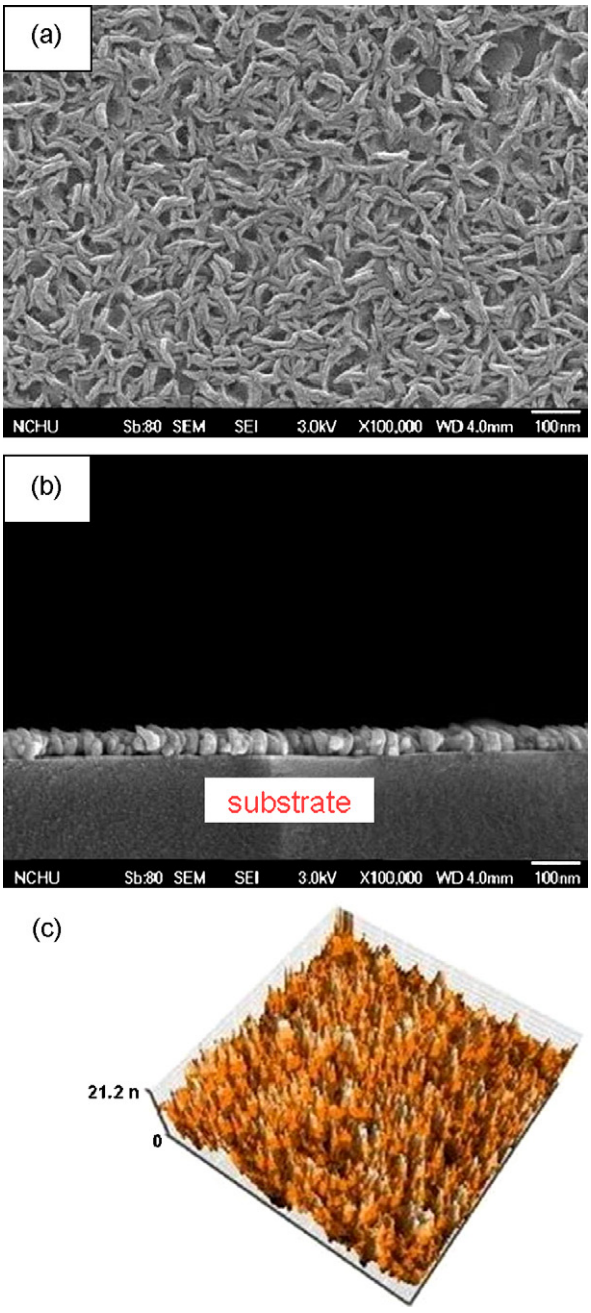

Fig. 3. (a) Top-down view of SEM image for dried precursor coated on glass substrate, (b) Side-view of SEM image for ZnO seed layer deposited on substrate, and (c) AFM graph of ZnO seed layer deposited on substrate.

be attributed to the characteristic stretching of the Zn–O bond [19]. A comparison between Figs. 2(b) and (c) indicates that the characteristic ZnO band became more distinct, consistent with the hydrothermal growth of the ZnO phase, and in agreement with our XRD analysis data.

Fig. 3(a) presents a top-down view of the SEM image of the precursor sol after it had been coated onto the substrate and dried by spin coating. A sheet-like structure was apparent on the substrate, identified by XRD as LBZA. Fig. 3(b) shows the side view of the SEM image of the ZnO seed layer deposited on the substrate, which was composed of uniform, discrete and upright grains with a height of ~20 nm. AFM graph (Fig. 3(c)) shows that the surface root-mean-square roughness of the seed layer is about 15 nm, confirming a rugged surface morphology. It was thought that such a morphological feature might be beneficial for the subsequent growth of rod arrays by the hydrothermal treatment.

Fig. 4 shows the top-down view and cross-sectional SEM images of the arrays following hydrothermal treatment under 130 °C for 4 h. The ZnO nanorods grew erectly and uniformly with a population density of $\sim 10^{10}$ cm^{-2} on the substrate. The diameter of the ZnO rods was 25–75 nm with an aspect ratio that ranged from 10 to 50. Based on our preliminary experiments, it should be noted that the seed layer could develop into rod arrays when the hydrothermal temperature was higher than 120 °C. The rod dimensions increased greatly with increasing temperature. As the temperature exceeded 160 °C, however, the as-grown rods contacted with each other and even coalesced together, resulting in the formation of undesired morphology. This result, coupled with the consideration for processing economy, the temperature of 130 °C was thus chose for hydrothermal treatment in this work.

Fig. 5 shows a typical TEM image of a single ZnO nanorod scraped from the sample shown in Fig. 4. The insets in Fig. 5 show the lattice fringes and corresponding SAED patterns for the bright and dark regions of the ZnO nanorod. Clear and regular lattice fringes can be observed, indicating a uniform crystalline structure without dislocations and stacking faults. Both the lattice spacing were found to be close to 0.26 nm, which corresponds to the distance between two adjacent (0 0 2) planes in the ZnO crystal, revealing that the ZnO nanorod preferentially grew in the *c*-axis direction, consistence with the XRD results. As evidenced by the same dotted SAED patterns from the two contrasting regions, the bright and dark parts in the ZnO nanorod possessed the same structure as a single crystal, which is similar to the previous study reported by Yi et al. [3]. This result may be served as an indirect evidence for that

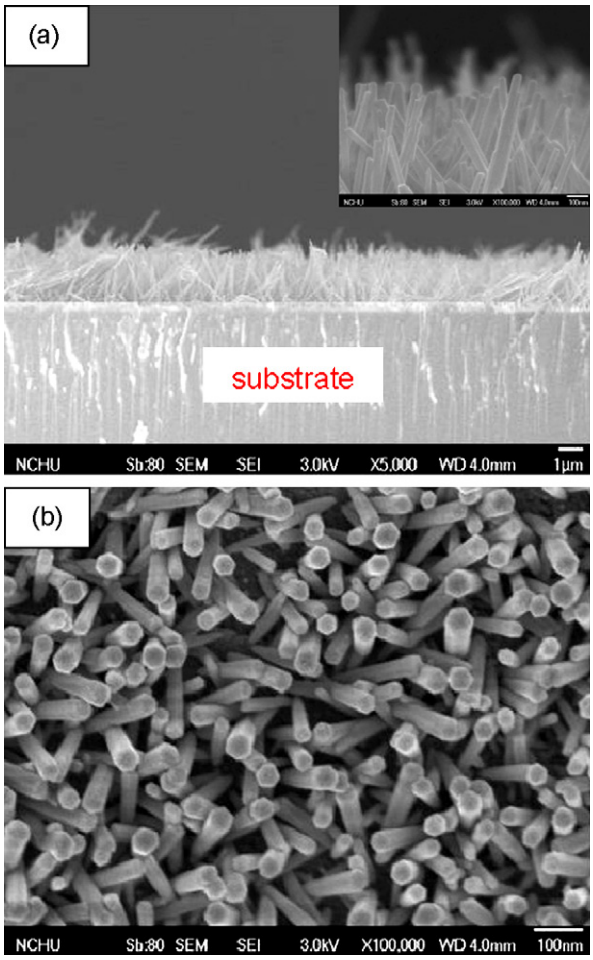

Fig. 4. (a) Cross-sectional and (b) top-down SEM images for ZnO nanorods hydrothermally grown at 130 °C for 4 h.

the contrast in the ZnO nanorod is likely due to strain, as proposed by Djurišić et al. [4].

Fig. 6 shows the PL spectra obtained at room temperature for the glass substrate, ZnO seed layer, and ZnO nanorods that were

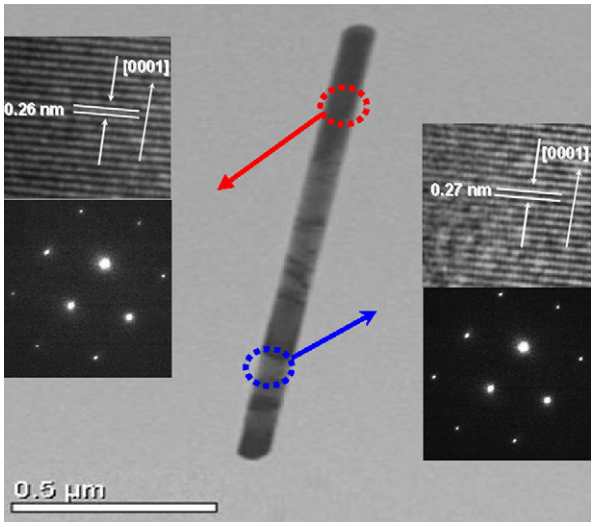

Fig. 5. Typical TEM photograph of a single ZnO nanorod grown hydrothermally at 130 °C for 4 h, scraped from the sample shown in Fig. 4; insets show the lattice fringes and corresponding SAED patterns for contrasting regions.

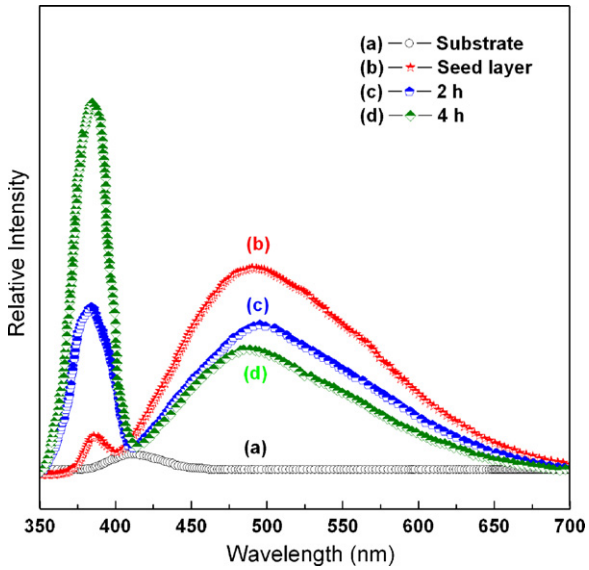

Fig. 6. Room-temperature PL spectra for (a) glass substrate, (b) ZnO seed layer, and ZnO nanorods grown hydrothermally at 130 °C for (c) 2 h and (d) 4 h.

hydrothermally grown for 2 or 4 h. The PL spectra of the ZnO seed layer and the as-grown ZnO nanorods exhibited two obvious emission peaks, a narrow UV emission (located at ~380 nm) and a broad green one (centered at ~500 nm). The low PL intensity for the ZnO seed layer was due to its extremely thin thickness. The UV emission increased in intensity while the intensity of the green luminescence decreased with the longer hydrothermal times.

4. Discussion

Recently, many research efforts have attempted to prepare directionally oriented ZnO thin films using sol–gel process (referred as the thin-film process), for which $ZnAc_2$ and MEA are commonly used and dispersed/dissolved in an alcohol (such as methanol, 2-methoxyethanol, or isopropanol) to form a precursor sol. As previously reported [16], the precursor sol derived from the alcoholic solution of $ZnAc_2$ and MEA can be transformed into LBZA after removal of the solvent. Moreover, the thermal decomposition of LBZA can occur with preheating, thus resulting in the production of ZnO accompanied by gaseous species such as CO_2 and H_2O. Since the (0 0 2) plane is associated with the lowest free energy in the wurtzite-structured ZnO [17], the crystalline arrangement for both the heterogeneous nucleation of the as-deposited ZnO on substrates and its subsequent growth/coalescence are mainly in the direction of [0 0 0 2], i.e., along the *c*-axis. Therefore, both higher concentrations of starting materials (generally ≥0.5 M) and repeating the coating and preheating procedures several times (usually spin coating and heating at 300 °C for 10 min, six repetitions) are required in the thin-film process to yield thin films of sufficient thickness (≥500 nm). In the present study; arrayed ZnO nanorods were successful prepared for the first time using the same regents, i.e., $ZnAc_2$ and MEA, but with several modifications including lower concentrations of reagents in both the ethanolic and aqueous solutions, fewer repetitions of the cycle from spin coating to preheating, and the use of an aqueous solution with a higher surface tension for hydrothermal growth.

Based on the XRD and FTIR analyses (Figs. 1 and 2), the formation mechanism of the sol–gel-derived ZnO seed layer coincides with that of the thin-film process mentioned above. However, the relatively lower concentrations of $ZnAc_2$ and MEA in ethanolic solution, coupled with double repetitions of the coating and preheating procedures, resulted in a rugged layer composed of discrete ZnO

grains deposited on the substrates (see Fig. 2(b) and (c)). These results are very different from the thin films that exhibit an even and continuous microstructure.

Previous research [3,6,14] has revealed that, without seeds, ZnO rods/wires that are hydrothermally grown on Si wafers, quartz glass and other amorphous materials are generally poorly aligned and exhibit low population density. The ZnO seed layer is believed to prefer the *c*-axis orientation for the growth of arrayed ZnO rods [20]. At Present, we can only speculate about the possible formation mechanism for the ZnO nanorods in our hydrothermal process. During the initial stage of aqueous solution preparation, MEA acts as a bidentate ligand to Zn^{2+}, rendering the solution stable against precipitation [14]. In addition, MEA is also a base [20], whose nucleophilic reaction with water generates OH^- ions that combine with Zn^{2+} to form $Zn(OH)_2$ as the hydrothermal treatment to proceed. This hypothesis is supported by the observed decrease in pH of the aqueous solution from ~8.6 at the beginning to ~7.3 at the end of the 4-h-hydrothermal treatment. At a temperature of above 125 °C, ZnO may be produced through the following chemical reaction [21]: $Zn(OH)_2 \rightarrow ZnO + H_2O$. However, the colloidal $Zn(OH)_2$ medium is difficult to collect and to analyze with XRD, perhaps due to its ultra-tiny size and amorphous nature. In fact, a hydrothermal temperature of ≤120 °C may hindered growth of the ZnO seeds, as confirmed by other experiments in this study and consistent with the conclusions of Sharikov et al. [22]. On the other hand, a temperature gradient exists in the fluid field in the hydrothermal/solvothermal processes, even though the temperature is set to a constant value, which in turn may cause natural convection and thereby induce mass-transfer. Consequently, the growth of ZnO seeds may take place *via* a typical phenomenon of Oswald ripening [23] by coalescence of the ZnO colloids derived from the above reaction, thus resulting in the formation of the arrayed ZnO nanorods. The aqueous solution usually exhibits a higher surface tension than the alcoholic solutions, which corresponds to limited abilities in terms of wetting and infiltration. The rugged seed layer immersed in the aqueous solution may be advantageous for inducing growth of the ZnO nanorods through the hydrothermal process due to the presence of fewer interfaces between the ZnO seeds and the aqueous solution. Also, the low concentrations of $ZnAc_2$ and MEA in the aqueous solution may repress the sudden formation of numerous ZnO colloids/nuclei, thus inhibiting the uncontrollable growth of ZnO nanorods. These might be contributing factors in explaining why the resultant products were not ZnO thin films or particles, but instead were arrayed nanorods in this study.

In general, ZnO nanostructures fabricated by hydrothermal methods are expected to exhibit a large number of defects due to the lower growth temperatures [8]. As shown in the PL spectra for our ZnO nanorods (Fig. 6), the UV emission (~3.37 eV), which is close to the theoretical band gap of ZnO, is due to the recombination of the free excitons [4]. The green emission, the most common intrinsic defect emission generated during ZnO preparation, is often attributed to the transition between the photoexcited hole and the ionized oxygen vacancy V_O^+ [24]. With a longer hydrothermal time, the exciton emission in the UV region was shown to increase in intensity while the intensity of the defect-related green luminescence decreased, suggesting an improvement in the crystalline quality of the ZnO nanorods. This inference could be supported by XRD analysis (Fig. 1).

5. Conclusion

For the first time, arrayed ZnO nanorods were successfully prepared on glass substrates at a low temperature *via* a wet chemical method using $ZnAc_2$ and MEA as raw materials The synthesis process included two steps, i.e., formation of the ZnO seed layer through a sol–gel approach and the induced growth of aligned nanorods *via* a hydrothermal route. As identified by instrumental analyses, the ZnO nanorod was confirmed to be single crystalline and was shown to grow along the *c*-axis. The PL measurements for the oriented ZnO nanorods exhibited a sharp UV emission peak at ~380 nm and a broad green emission band centered at ~500 nm at room temperature. Moreover, the crystallinity and optical properties of the ZnO nanorods seemed to improve with increased hydrothermal time. This process does not require the use of specialty reagents, complex procedures or expensive equipment. It is suggested that our approach could potentially serve as an alternative means of fabricating arrayed ZnO nanorods for applications in opto-electronic and other devices. Since the product characteristics (morphology, population density, optoelectronic properties) may have been influenced by other parameters (such as the concentrations of $ZnAc_2$ and MEA in ethanolic solution for seeding, the aqueous solution concentration for nanorod growth, and the temperature of hydrothermal process), further optimization using the Taguchi method [25] is currently being undertaken in our laboratory to obtained higher-quality arrayed ZnO nanorods.

Acknowledgement

Financial support from the National Science Council of the Republic of China (Taiwan) under grant number NSC 97-2221-E-606 -022 is gratefully acknowledged.

References

[1] Ü. Özgür, Y.I. Alivov, C. Liu, A. Teke, M.A. Reshchikov, S. Doğan, V. Avrutin, S.J. Cho, H. Morkoç, Journal of Applied Physics 98 (2005) 041301–041306.
[2] S.J. Pearton, D.P. Norton, K. Ip, Y.W. Heo, T. Steiner, Progress in Materials Science 50 (2005) 293–340.
[3] S.-H. Yi, S.-K. Choi, J.-M. Jang, J.-A. Kim, W.-G. Jung, Journal of Colloid and Interface Science 313 (2007) 705–710.
[4] A.B. Djurišić, Y.H. Leung, Small 2 (2006) 944–961.
[5] L. Vayssieres, Advanced Materials 15 (2003) 464–466.
[6] L.E. Greene, M. Law, J. Goldberger, F. Kim, J.C. Johnson, Y. Zhang, R.J. Saykally, P. Yang, Chemie International Edition 42 (2003) 3031–3034.
[7] Y.G. Wang, C. Yuen, S.P. Lau, S.F. Yu, B.K. Tay, Chemical Physics Letters 377 (2003) 329–332.
[8] W.M. Kwok, A.B. Djurišić, Y.H. Leung, D. Li, K.H. Tam, D.L. Phillips, W.K. Chan, Applied Physics Letters 89 (2006) 183112–183113.
[9] Z. Wang, X.-f. Qian, J. Yin, Z.-k. Zhu, Langmuir 20 (2004) 3441–3448.
[10] M. Huang, Y. Wu, H. Feick, N. Tran, E. Weber, P. Yang, Advanced Materials 13 (2001) 113–116.
[11] M. Rosina, P. Ferret, P.-H. Jouneau, I.-C. Robin, F. Levy, G. Feuillet, M. Lafossas, Microelectronics Journal 40 (2009) 242–245.
[12] Y.H. Leung, A.B. Djurišić, M.H. Xie, Journal of Crystal Growth 284 (2005) 80–85.
[13] Y.-S. Kim, W.-P. Tai, S.-J. Shu, Thin Solid Films 491 (2005) 153–160.
[14] C.-Y. Zhang, X.-M. Li, X. Zhang, W.-D. Yu, J.-L. Zhao, Journal of Crystal Growth 290 (2006) 67–72.
[15] P. Sagar, P.K. Shishoda, R.M. Mehra, H. Okada, A. Wakahara, A. Yoshida, Journal of Luminescence 126 (2007) 800–806.
[16] E. Hosono, S. Fujihara, T. Kimura, H.J. Imai, Journal of Colloid and Interface Science 272 (2004) 391–398.
[17] S. Fujihara, C. Sasaki, T. Kimura, Applied Surface Science 180 (2001) 341–350.
[18] L.G. Wade Jr., Organic Chemistry, 6th ed., Pearson Education, Inc., New Jersey, USA, 2006, pp. 1251–1252.
[19] S. Musić, Đ. Dragčević, M. Maljković, S. Popović, Materials Chemistry and Physics 77 (2002) 521–530.
[20] M.J. O'Neil (Ed.), The Merck Index, 13th ed., Merck & Co., Inc., New Jersey, USA, 2001, p. 664.
[21] McGraw-Hill's AccessScience, http://www.accessscience.com/overflow.aspx?searchStr=Zinc&stype=4&term=Zinc&rootID=798443&p=2.
[22] F.Yu. Sharikov, V.K. Ivanov, Yu.D. Tret'yakov, Doklady Chemistry 410 (2006) 185–188.
[23] C. Pacholski, A. Kornowski, H. Weller, Angewandte Chemie International Edition 41 (2002) 1188–1191.
[24] K. Vanheusden, C.H. Seager, W.L. Warren, D.R. Tallant, J.A. Voigt, Applied Physics Letters 68 (1996) 403–405.
[25] G. Taguchi, Y. Yokoyama, Y. Wu, Taguchi Methods/Design of Experiments, American Supplier Institute (ASI) Press, Tokyo, Japan, 1993.